# Structural analysis of interfacial layers in Ti/Ta/Al ohmic contacts to *n*-AlGaN

S.-H. Lim,[a] W. Swider, J. Washburn, and Z. Liliental-Weber
*Materials Science Division, Lawrence Berkeley National Laboratory, Berkeley, California 94720*

(Received 24 May 2000; accepted for publication 13 September 2000)

Detailed structure of the interfacial layers of Ti/Ta/Al ohmic contacts to *n*-type AlGaN/GaN/sapphire are investigated by means of transmission electron microscopy. High-resolution electron microscopy (HREM), optical diffractograms, and computer simulations confirmed that TiN (~10.0 nm) and $Ti_3AlN$ (~1.4 nm) interfacial layers form at the interface between the Ti layer and the $Al_{0.35}Ga_{0.65}N$ substrate by a solid state reaction during annealing for 3 min in $N_2$ at 950 °C. The orientation relationship between $Ti_3AlN$ and $Al_{0.35}Ga_{0.65}N$ was found to be: $[011]_{Ti_3AlN} \| [2\bar{1}\bar{1}0]_{Al_{0.35}Ga_{0.65}N}$ and $(1\bar{1}\bar{1})_{Ti_3AlN} \| (0001)_{Al_{0.35}Ga_{0.65}N}$. The cubic $Ti_3AlN$ interfacial layer has a lattice parameter of $0.411 \pm 0.003$ nm with the space group $Pm3m$ matching that of $Al_{0.35}Ga_{0.65}N$. A model of the atomic configurations of the $Ti_3AlN/Al_{0.35}Ga_{0.65}N$ interface is proposed. This model is supported by a good match between the simulated and the experimental HREM image of the $Ti_3AlN/Al_{0.35}Ga_{0.65}N$ interface. The formation of TiN and $Ti_3AlN$ interfacial layers appears to be responsible for the onset of the ohmic contact behavior in Ti/Ta/Al contacts.
 [S0021-8979(00)04924-0]

## I. INTRODUCTION

Recently, GaN-based semiconductors have been the subject of intensive research for both optoelectronic devices and high-temperature/high-power electronic devices including light emitting diodes[1,2] in the blue–green and ultraviolet wavelength region. The reliability, reproducibility, and long term stability under extreme (high temperature) operating conditions are very important considerations in the selection of the ohmic metal contacts on GaN in the fabrication of devices such as metal–semiconductor heterostructure field-effect transistor (HFET).[3] In particular, performance of devices like $p-n$ junction GaN light-emitting diodes is known to depend on the contact resistance.[4–7] Development of a stable low resistance ohmic contact for GaN is thus of great importance.

In the case of GaN, the Fermi level is unpinned at the surface, hence, ohmic contact formation to GaN (and/or AlGaN) can be determined based on the work function of the metal system. There are several reports[4–9] on ohmic contacts to *n*-type GaN with varying results. Of all the metal systems proposed, the Ti/Al metal system, which displayed the lowest contact resistivity to *n*-type GaN (and/or AlGaN), is presently the most widely used. A TiN layer has been observed[4] at the interface of Ti/Al and Ti/Al/Ni/Au contacts annealed at 900 °C. Many researchers have suggested[6,8,9] that due to the formation of a TiN layer when Ti reacts with GaN, a high concentration of nitrogen vacancies is created near the interface, causing the GaN to be heavily doped *n*-type. Furthermore, Ruvimov *et al.*[7] reported that a 15–25-nm-thick interfacial $AlTi_2N$ layer was observed at the Ti/Al/*n*-type AlGaN interface. However, understanding of the mechanism which causes ohmic contact formation on *n*-GaN (and/or *n*-AlGaN) is not yet clear. Thus, further detailed structural studies are necessary for better understanding of this ohmic contact formation.

In this study, we focused on the structural characteristics of the interfacial layers and interfaces in Ti/Ta/Al metal contacts to *n*-AlGaN/GaN/sapphire. Transmission electron microscopy (TEM), especially, high-resolution electron microscopy (HREM), due to its extremely fine spatial resolution and the ability to obtain crystallographic information from small areas, allowed us to investigate details of the microstructure that are not apparent by other techniques. Also, the HREM images were evaluated by comparing the micrographs with simulated images. Detailed structural models of the interface between the interfacial layer and the substrate have to be assumed in order to simulate the images.

## II. EXPERIMENT

Typical AlGaN/GaN HFET structures grown by metal-organic chemical vapor deposition at 1040 °C (pure GaN) or 1100 °C (AlGaN) on (0001) sapphire substrates have a 1-$\mu$m-thick insulating GaN layer followed by a 3-nm-thick undoped AlGaN layer and a 30-nm-thick doped AlGaN layer. The HFET samples were first etched with reactive ion etching using $CCl_2F_2$ to form mesa structures. The samples were cleaned in organic solvents, followed by etching in a HCl:HF:$H_2O$ solution, and blown dry. Details of the metallization schemes are reported elsewhere.[10] The structure of Al/Ta/Ti/AlGaN/GaN/sapphire used in this work is shown in Fig. 1. The samples were annealed in a $N_2$ ambient at 950 °C for 3 min using rapid thermal annealing. Contact resistance was measured by the transmission line method.

The structural characteristics of the layers on an atomic scale were investigated using a JEM-ARM 800 electron mi-

[a]Author to whom correspondence should be addressed; electronic mail: shlim@lbl.gov

 

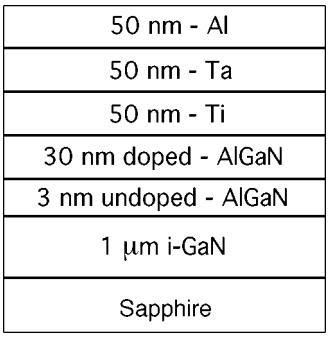


FIG. 1. Structure of Al/Ta/Ti/AlGaN/GaN/sapphire substrate used in this work.

croscope operating at 800 kV. The point-to-point resolution of the electron microscope is estimated to be 0.16 nm. A series of simulated images using the Mac Tempas program[11] were obtained for the interface structure between the interfacial layer and AlGaN. The parameters for the JEM-ARM 800 electron microscope used in the image simulation are as follows: spherical aberration coefficient $C_S = 1.95$ mm; beam divergence semiangle $\alpha = 3.3$ mrad; and Gaussian defocus spread half width $\Delta = 0.84$ nm. The atomic scattering factors used were those of neutral atoms. The compositional analyses of the AlGaN layer after annealing were performed using a Philips CM200 (200 kV) field emission gun TEM equipped with an ultrathin window and an Oxford energy dispersive x-ray (EDX) spectrometer.

## III. RESULTS AND DISCUSSION

### A. Morphology and orientation relationships

Figure 2 shows a bright field cross-sectional TEM image of a Ti/Ta/Al layer on the AlGaN/GaN HFET substrate. The strain contrast, as indicated by arrows, at the metal–semiconductor interface shows the existence of a second phase, suggesting that diffusion of the metal elements at the interface occurred during annealing, leading to the formation of a compound interfacial layer. The image shows that the AlGaN/Ti interface is very rough. Figure 3 shows a cross-sectional HREM image. The incident electron beams were parallel to the $[2\bar{1}\bar{1}0]_{GaN}$ direction. The interface between the AlGaN and the GaN HFET substrate is quite smooth and free of any interfacial phases. Well-defined atomic rows and lattice planes can be identified. An EDX analysis of the AlGaN layer indicates the composition of $Al_xGa_{1-x}N$ with

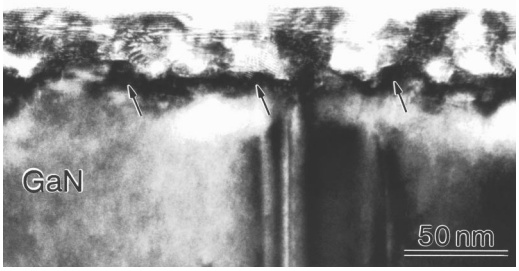


FIG. 2. Cross-sectional bright field image of Ti/Ta/Al thin layers on AlGaN/GaN substrate.

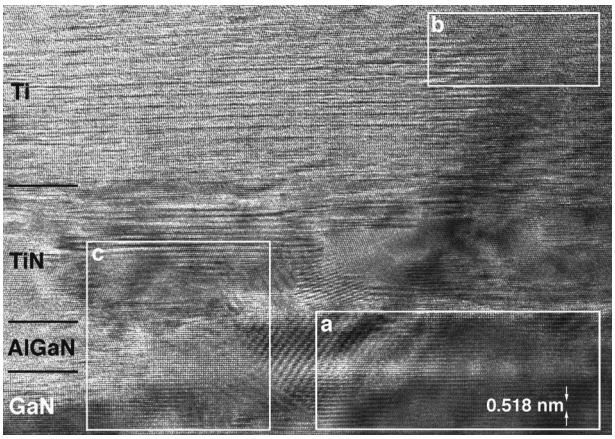


FIG. 3. HREM image of the metal contact layers on AlGaN/GaN HFET substrate.

the $x \fallingdotseq 0.35$, slightly higher than this expected from a crystal grower, $x \fallingdotseq 0.23$. Figure 4(a) shows an enlarged image of the strain contrast features, similar to what would be expected from an array of misfit dislocations. This contrast is due to local fluctuation of Al composition that would be consistent with EDX data. It is believed that this local fluctuation of Al composition in the AlGaN affected the metal contacts properties.

Figure 4(b) shows an enlarged image of the area above the interfacial area, corresponding to the white rectangular region (b) in Fig. 3. The arrangement of the lattice planes and the angles between these planes agree with a Ti lattice image, suggesting that not all the Ti reacted with the AlGaN during annealing. The Ti layer, as shown by a white line in Fig. 4(b), is often in a twined orientation.

Figure 4(c) shows an enlarged image of the interfacial layer region, corresponding to the white rectangular region (c) in Fig. 3. A cubic TiN phase ($a = 0.424$ nm) with a ~10 nm thickness between the Ti layer and the $Al_{0.35}Ga_{0.65}N$ has been found using the measured interplanar distances and angles of the Ti-rich layer in the HREM image of Fig. 4(c). This formation of a TiN layer is consistent with previous reports.[4,6–8]

The orientation relationship between TiN and $Al_{0.35}Ga_{0.65}N$ was found to be: $(111)_{TiN} \| (0001)_{Al_{0.35}Ga_{0.65}N}$ and $[\bar{2}11]_{TiN} \| [11\bar{2}0]_{Al_{0.35}Ga_{0.65}N}$. In addition to the TiN layer, a $Ti_3AlN$ layer with a distinctly different image can be observed between the TiN layer and the $Al_{0.35}Ga_{0.65}N$ substrate in HREM images. The orientation relationship between the $Ti_3AlN$ layer and the $Al_{0.35}Ga_{0.65}N$ substrate has been observed as: $[011]_{Ti_3AlN} \| [2\bar{1}\bar{1}0]_{Al_{0.35}Ga_{0.65}N}$ and $(1\bar{1}\bar{1})_{Ti_3AlN} \| (0001)_{Al_{0.35}Ga_{0.65}N}$. In Secs. III B and III C, we discuss the formation of interfacial layers and the atomic structure at the $Ti_3AlN/Al_{0.35}Ga_{0.65}N$ interface based on the above orientation relationships and the HREM images.

### B. Formation of interfacial phases

To identify the thin ternary layer, we carried out the estimation of interplanar distances and angles in this layer. We found a cubic $Ti_3AlN$ phase ($a = 0.411$ nm) with a thick-

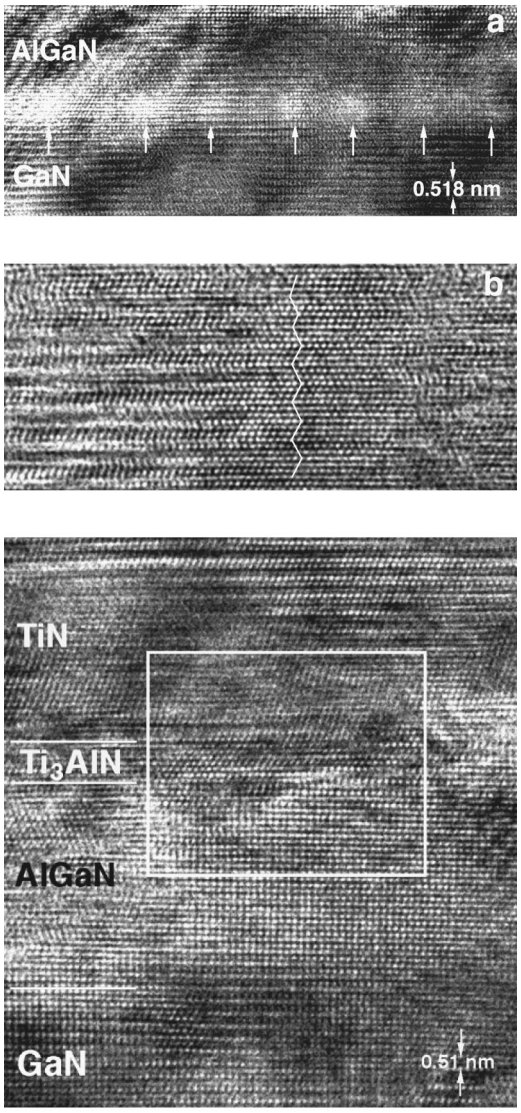


FIG. 4. Enlarged image of the interface between AlGaN and GaN (a), Ti layer (b), and interface between TiN and AlGaN (c), corresponding to the white rectangular regions (a), (b), and (c) in Fig. 3.

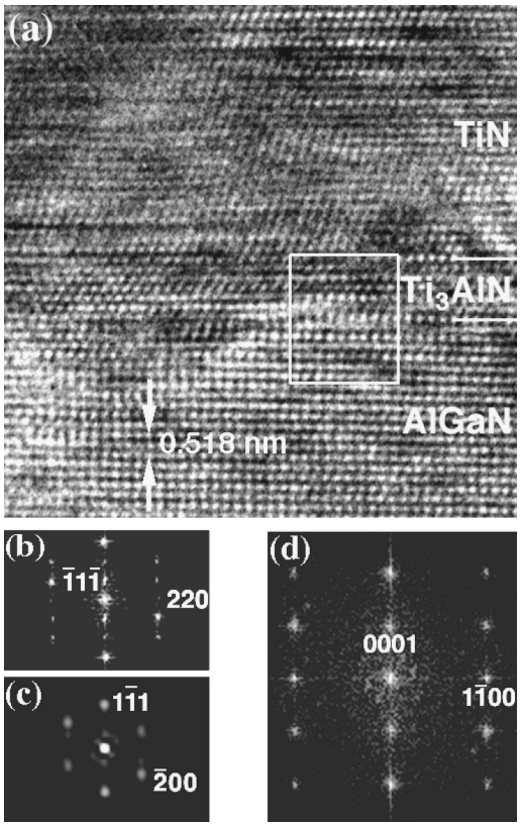


FIG. 5. (a) Enlarged image of the interface layers, corresponding to the white rectangular region in Fig. 4(c). (b), (c), and (d) are power spectra obtained from TiN (b), $Ti_3AlN$ (c), and AlGaN (d). Corresponding zone axes were $[\bar{1}12]_{TiN}$ (b), $[011]_{Ti_3AlN}$ (c), $[2\bar{1}\bar{1}0]_{AlGaN}$ (d), respectively.

ness of ~1.4 nm. Figure 5(a) shows an enlarged image of the interface region between TiN and $Al_{0.35}Ga_{0.65}N$, corresponding to the white rectangular region in Fig. 4(c). Figures 5(b), 5(c), and 5(d) show the optical diffractograms of the perfect regions in the TiN, $Ti_3AlN$, and $Al_{0.35}Ga_{0.65}N$. The lattice parameters of the reaction products, as evaluated from the optical diffractogram, agree with the lattice constants of TiN, $Ti_3AlN$, and $Al_{0.35}Ga_{0.65}N$, respectively. Consequently, the HREM observations and optical diffractograms from the Al/Ta/Ti/$Al_{0.35}Ga_{0.65}N$ interface regions confirm that Ti has reacted with $Al_{0.35}Ga_{0.65}N$ at the interface, resulting in the formation of TiN and $Ti_3AlN$ layers. Since the $Ti_3AlN$ layer is very thin and the interface is undulated, we cannot be sure if the layer is continuous or if it forms islands.

### C. Structure models of ternary interfacial phase

A structural model of the interface has to be assigned in order to be able to simulate the images. Image simulation of the interface and comparison with the experimentally observed image is therefore a useful method to develop a possible interface structure model.[12] In order to obtain information about the atomic configuration at the $Ti_3AlN$ layer/$Al_{0.35}Ga_{0.65}N$ interface, image simulations are performed based on hypothetical interfacial structure models suggested by the HREM image. First, the following orientation relationship between $Ti_3AlN$ layer and $Al_{0.35}Ga_{0.65}N$ substrate has been observed; $[011]_{Ti_3AlN} \| [2\bar{1}\bar{1}0]_{Al_{0.35}Ga_{0.65}N}$ and $(1\bar{1}\bar{1})_{Ti_3AlN} \| (0001)_{Al_{0.35}Ga_{0.65}N}$. Second, the composition of the Al in AlGaN appears to be different than that assigned by the crystal grower, i.e., $Al_{0.35}Ga_{0.65}N$ instead of $Al_{0.23}Ga_{0.77}N$. Finally, since the interplanar spacing for $\{111\}_{Ti_3AlN}$ should be 0.237 nm, the calculations were performed for interplanar distances in the range 0.225–0.245 nm. $Ti_3AlN$ belongs to space group $Pm3m$ (space group No. 221) and the crystal structure has a cubic lattice. In order to derive reliable atomic positions, computer simulations and adjustment of atomic positions were repeated until the best fit was obtained with the observed HREM image. In order to perform the computer simulations of the interface, a supercell based on the structural model of the interface was built up. We investigated the interface structure between the $Ti_3AlN$ layer and $Al_{0.35}Ga_{0.65}N$ substrate by comparing the micrographs with simulated images. Figures 6(a) and 6(b) show projections of the interface model and the supercell of the $Ti_3AlN/Al_{0.35}Ga_{0.65}N$ interface along the

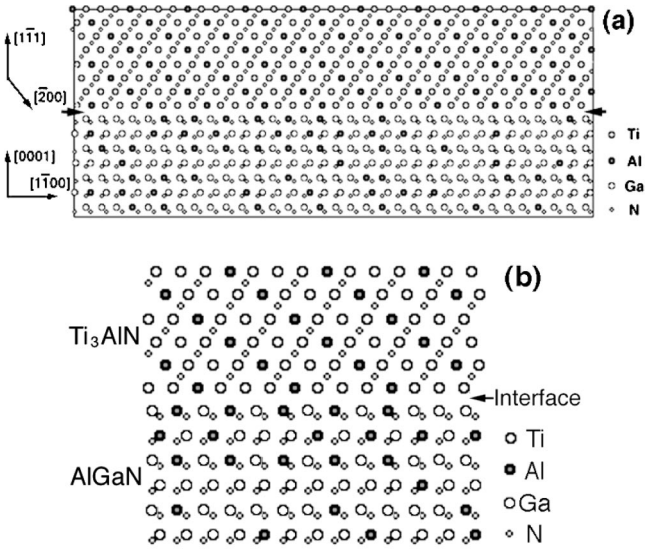


FIG. 6. (a) Proposed model of the interfacial area; (b) supercell for the image simulation proposed model. Small arrows indicate the interface.

$[011]_{Ti_3AlN}\|[2\bar{1}\bar{1}0]_{Al_{0.35}Ga_{0.65}N}$ direction. In Fig. 7, a comparison of this model with the experimental HREM image is shown. Figures 7(a), 7(b), 7(c), and 7(d) show the HREM image, the processed image obtained by the filtering method[13] of Fig. 7(a), the projected potential based on the supercell of Fig. 6(b), and the simulated image using the specimen thickness of 12.0 nm and a defocus $\Delta f$ of $-48.0$ nm. All figures are viewed along the $[011]_{Ti_3AlN}\|[2\bar{1}\bar{1}0]_{Al_{0.35}Ga_{0.65}N}$ direction. Simulated images of the interface structure model of the $Ti_3AlN/Al_{0.35}Ga_{0.65}N$ [Fig. 7(d)] showed satisfactory agreement with the experimental HREM image [Fig. 7(a)]. The atomic columns containing metal ions appear as white spots shown on Figs. 7(c) and 7(d). There are good matches between experimental and simulated images in electron beam directions [Figs. 7(a) and 7(d)] thus confirming the basic correctness of the structural model for the $Ti_3AlN/Al_{0.35}Ga_{0.65}N$ interface.

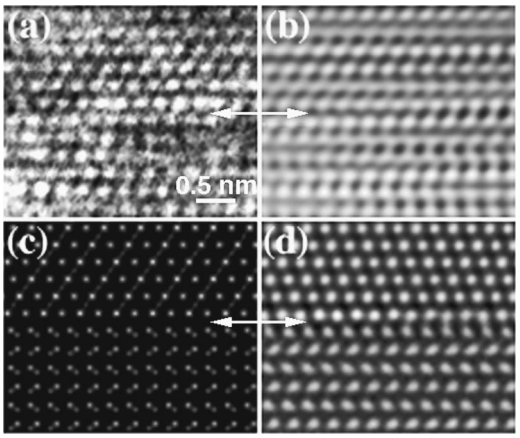


FIG. 7. Comparison between experimental and calculated images: (a) experimental image, (b) inverse Fourier transformation image, (c) projected potential, and (d) calculated HREM image which is a good match with the observed area.

### D. The role of interfacial phases

Ruvimov *et al.*[7] reported that $Ti_2AlN$ and TiN interfacial phases were observed at the Ti/Al contact to *n*-AlGaN samples after annealing for 80 min at 950 °C with a specific contact resistance of $5.8\times10^{-4}\,\Omega\,cm^2$. We observe formation of $Ti_3AlN$ and TiN interfacial layers between Ti and $Al_{0.35}Ga_{0.65}N$ substrate of the metal contacts annealed for 3 min in $N_2$ at 950 °C. The measured contact resistance was $5.11\times10^{-4}\,\Omega\,cm^2$. This slight difference in contact resistance might be insignificant or might be related to the difference between formation of $Ti_2AlN$ or $Ti_3AlN$ phase at the interface for different annealing conditions. In this and earlier studies,[7] TiN was found at the interface and it is believed that a high concentration of N vacancies in the layer provides high electron concentrations,[3] which leads to low resistance of ohmic contacts. Due to reaction between the Ti and the AlGaN which is consumed, tunneling through this layer to GaN could take place. This would be similar to Fan *et al.*,[8] who suggested that at a TiN–GaN interfacial area bending of the GaN conduction band could be sufficient for tunneling. Therefore, the development of a low resistance contact using the Ti/Ta/Al metallization scheme suggests that control of interfacial reactions upon annealing at high temperatures is the most important factor for achieving low contact resistivity.

## IV. SUMMARY

Detailed structural analysis of the interface and interfacial layers at metal/AlGaN interfaces of Ti/Ta/Al ohmic contacts to *n*-type $Al_{0.35}Ga_{0.65}N$/GaN/sapphire was performed by TEM, HREM, optical diffractogram, and computer simulations. A thin layer of $Ti_3AlN$ (~1.4 nm) has been identified at the interface, in addition to the TiN layer. The orientation relationship between $Ti_3AlN$ and $Al_{0.35}Ga_{0.65}N$ was found to be: $[011]_{Ti_3AlN}\|[2\bar{1}\bar{1}0]_{Al_{0.35}Ga_{0.65}N}$ and $(1\bar{1}\bar{1})_{Ti_3AlN}\|(0001)_{Al_{0.35}Ga_{0.65}N}$. A structural model of the atomic configurations of the $Ti_3AlN/Al_{0.35}Ga_{0.65}N$ interface has been proposed. This model is supported by a good match between simulated and experimental HREM images of the $Ti_3AlN/Al_{0.35}Ga_{0.65}N$ interface. The formation of these interfacial layers appears to be responsible for the ohmic contact behavior in the Al/Ta/Ti/$Al_{0.35}Ga_{0.65}N$/GaN/sapphire heterostructure system.

## ACKNOWLEDGMENTS

This work was supported by the BMDO project (Dr. K. Wu) under Contract No. W31RPD-9-A9604 through the U.S. Department of Energy under Contract No. DE-AC03-76SF00098. The authors gratefully acknowledge collaboration with Professor S.S. Lau and D. Qiao of the Department of Electrical and Computer Engineering at University of California, San Diego and are grateful to them for providing the samples and for fruitful discussions. The use of the facilities at the National Center for Electron Microscopy at the Lawrence Berkeley National Laboratory is greatly appreciated.

[1] S. Nakamura, T. Mukai, and M. Senoh, Jpn. J. Appl. Phys., Part 2 **30**, L1998 (1991).
[2] S. N. Mohammad, A. Salvador, and H. Morkoç, Proc. IEEE **83**, 1306 (1995).
[3] M. A. Khan, A. R. Bhattarai, J. N. Kuznia, and D. T. Olson, Appl. Phys. Lett. **63**, 1214 (1993).
[4] S. Ruvimov, Z. Liliental-Weber, J. Washburn, K. J. Duxstad, E. E. Haler, Z.-F. Fan, S. N. Mohammad, W. Kim, A. E. Botchkarev, and H. Morkoç, Appl. Phys. Lett. **69**, 1556 (1996).
[5] B. P. Luther, S. E. Mohney, T. N. Jackson, M. A. Khan, Q. Chen, and J. W. Yang, Appl. Phys. Lett. **70**, 57 (1997).
[6] M. E. Lin, Z. Ma, F. Y. Huang, Z. F. Fan, L. H. Allen, and H. Morkoç, Appl. Phys. Lett. **64**, 1003 (1994).
[7] S. Ruvimov, Z. Liliental-Weber, J. Washburn, D. Qiao, S. S. Lau, and P. K. Chu, Appl. Phys. Lett. **73**, 2582 (1998).
[8] Z. F. Fan, S. N. Mohammad, W. Kim, Ö. Aktas, A. E. Botchkarev, and H. Morkoç, Appl. Phys. Lett. **68**, 1672 (1996).
[9] J. D. Guo, C. I. Lin, M. S. Feng, F. M. Pan, G. C. Chi, and C. T. Lee, Appl. Phys. Lett. **68**, 235 (1996).
[10] Q. Z. Liu, L. S. Yu, F. Deng, S. S. Lau, Q. Chen, J. W. Yang, and M. A. Khan, Appl. Phys. Lett. **71**, 1658 (1997).
[11] R. Kilaas, in *Proceedings of the 45th Annual Meeting of the Electron Microscopy Society of America, Baltimore*, 1987, edited by G. W. Bailey (San Francisco Press, San Francisco, CA, 1987), p. 66.
[12] J. C. H. Spence, *Experimental High-Resolution Electron Microscopy* (Oxford University Press, United Kingdom, 1988).
[13] D. Shindo and K. Hiraga, *High-Resolution Electron Microscopy for Materials Science* (Springer, Tokyo, 1998); Generally, in a digital diffractogram of a high-resolution image, the noise on the image forms a monotonic background with no sharp peaks. Thus, by selecting diffraction spots on a digital diffractogram and carrying out the inverse Fourier transform, this noise may be removed.